Supplementary material

Instrumentation figures

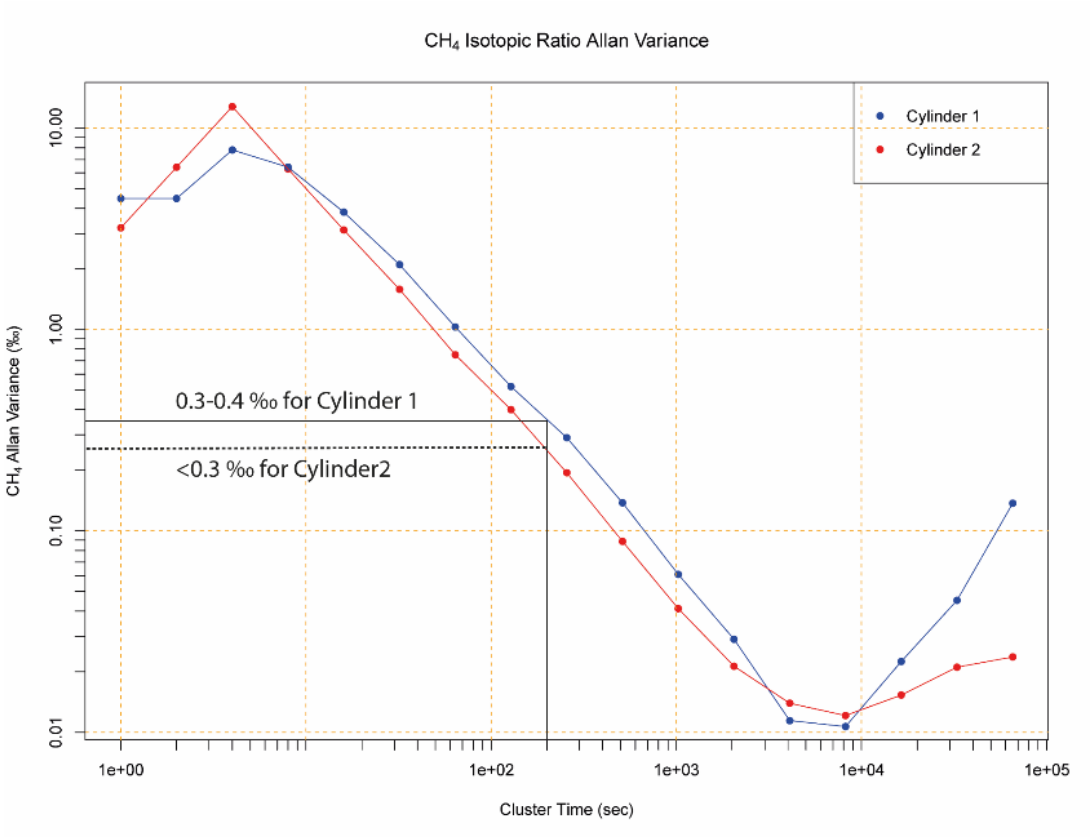

Figure S1: Allan variance of $\delta^{13}CH_4$ values for two working standards. Cylinder 1 and 2 are the low and high standard respectively. The vertical line denotes 4 minutes.

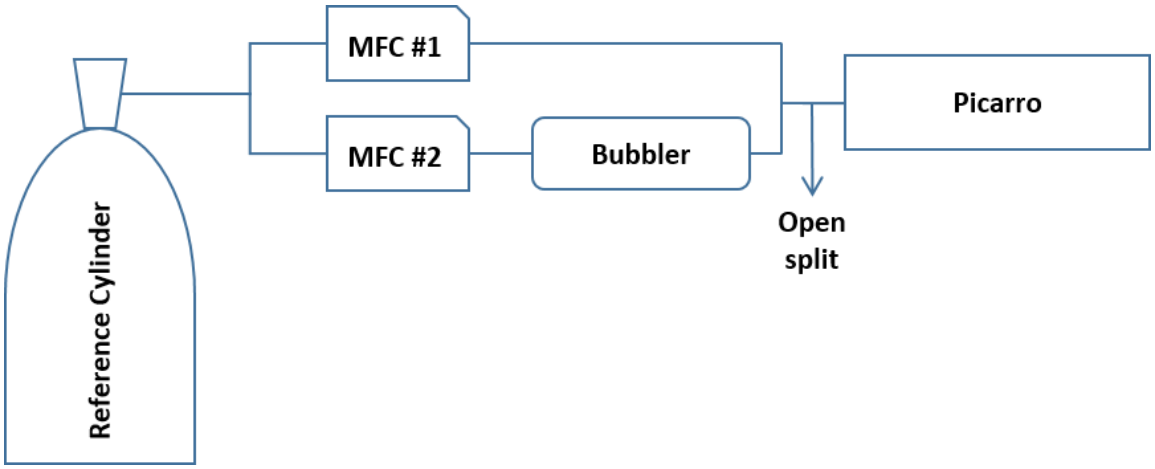

Figure S2: Experimental setup used for the water correction. The bubbler is a 1 litre stainless steel vessel filled with 0.3 litre of distilled water. The mass flow controller (MFC) is a red-y smart series meter (red-y GSC-B flow rate 0-1000 sccm).

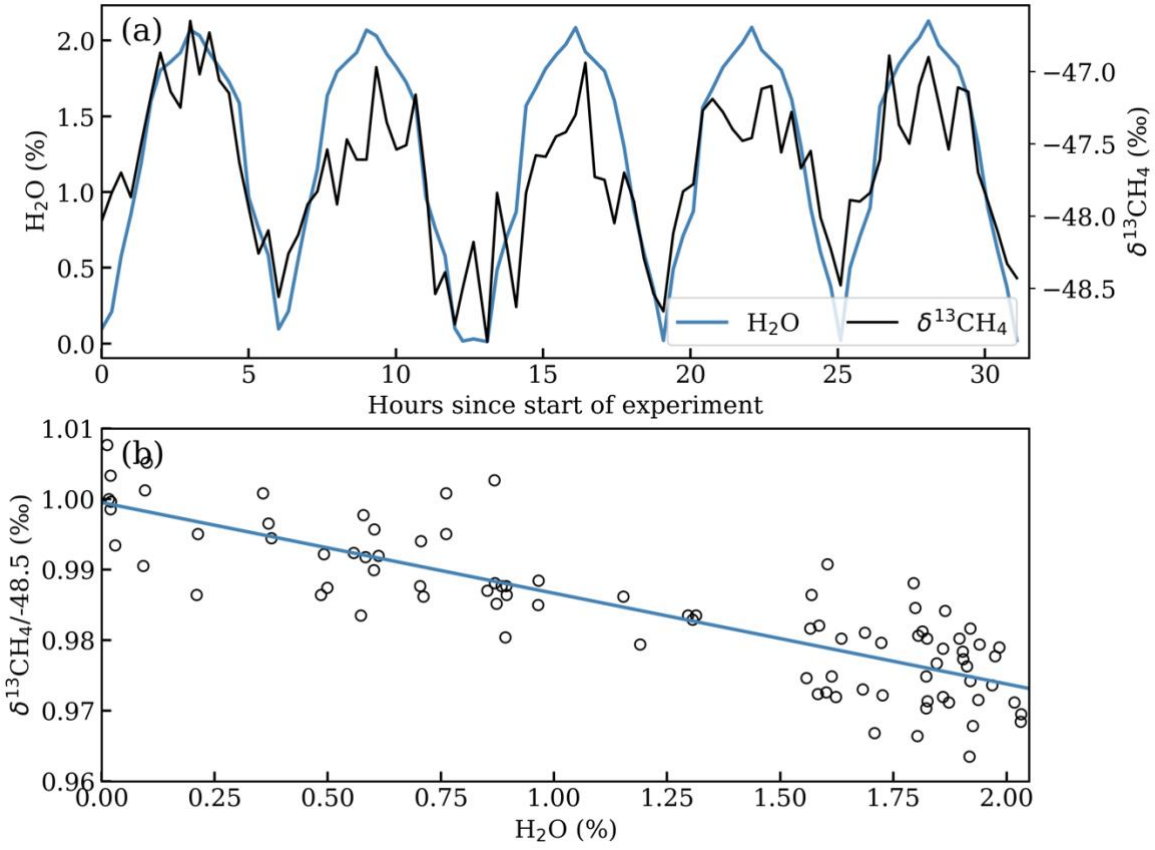

Figure S3: (a) $\delta^{13}CH_4$ values measured during the experiment to correct isotopic data for water vapour along with water concentration values; (b) regression line of the ratio of wet to dry $\delta^{13}CH_4$ values against the water concentration.

Approach for automated Keeling plot analysis

Our selection criteria for including a pollution event in the Keeling plot analysis considers the variation in mole fractions (i.e. the mole fraction peak strength) within a moving window. Considering variations in the $\delta^{13}CH_4$ potentially leads to pollution events with source signatures near background $\delta^{13}CH_4$ values being excluded in the analysis, as does using the correlation coefficient of a Keeling plot as a measure of the coherency of a pollution event.

To specify the magnitude of a pollution event for which δ_s could be well-characterised with the measurement uncertainty of our instrument we evaluated the recovery of an isotopic source signature in pseudo-data for peak strengths from 50 ppb to 300 ppb (increasing in 50 ppb increments; Fig S4). Ideal pollution events were constructed with a range of distinct isotopic signatures (-35 ‰, -40 ‰, -46 ‰ and, -65 ‰) using a mass balance approach with Gaussian white noise of 0.2 ‰ standard deviation added to represent measurement uncertainty. For each peak strength and isotopic signature 1000 simulations were run and the δ_s values determined. Larger variations in δ_s across simulations for pollution events with smaller peak strengths are seen (Fig. S4). Standard deviations of δ_s for simulated pollution events with the same peak strength but with different isotopic signatures are within 0.1 ‰, for peak strengths 150 ppb or larger (Table S1), of each other and decrease exponentially with increasing peak strength size (Fig. S5). Based on these simulations we considered pollution events of at least 100 ppb for which δ_s can be well-characterised with our measurement uncertainty.

Isotopic source values were calculated with ICL atmospheric measurements using peak strengths of 100, 150, and 200 ppb for 12 h, 3-day and 7-day moving windows. Whilst smaller peak strengths return a larger number of δ_s values, their mean standard error increases and the range of δ_s values include unrealistic values (Table S2). For the 3-day and 7-day windows, nearly three time the proportion of δ_s values between -30 ‰ and -35 ‰ are observed in the 100 and 150 ppb peak strengths in comparison to the 200 ppb δ_s values. For the 12 window we did not find large differences in the proportions of 12 h δ_s < -45 ‰ for the different peak strengths (Table S2) compared to the 3 and 7-day windows. Based on these analyses we opted for peak strengths of 150 ppb.

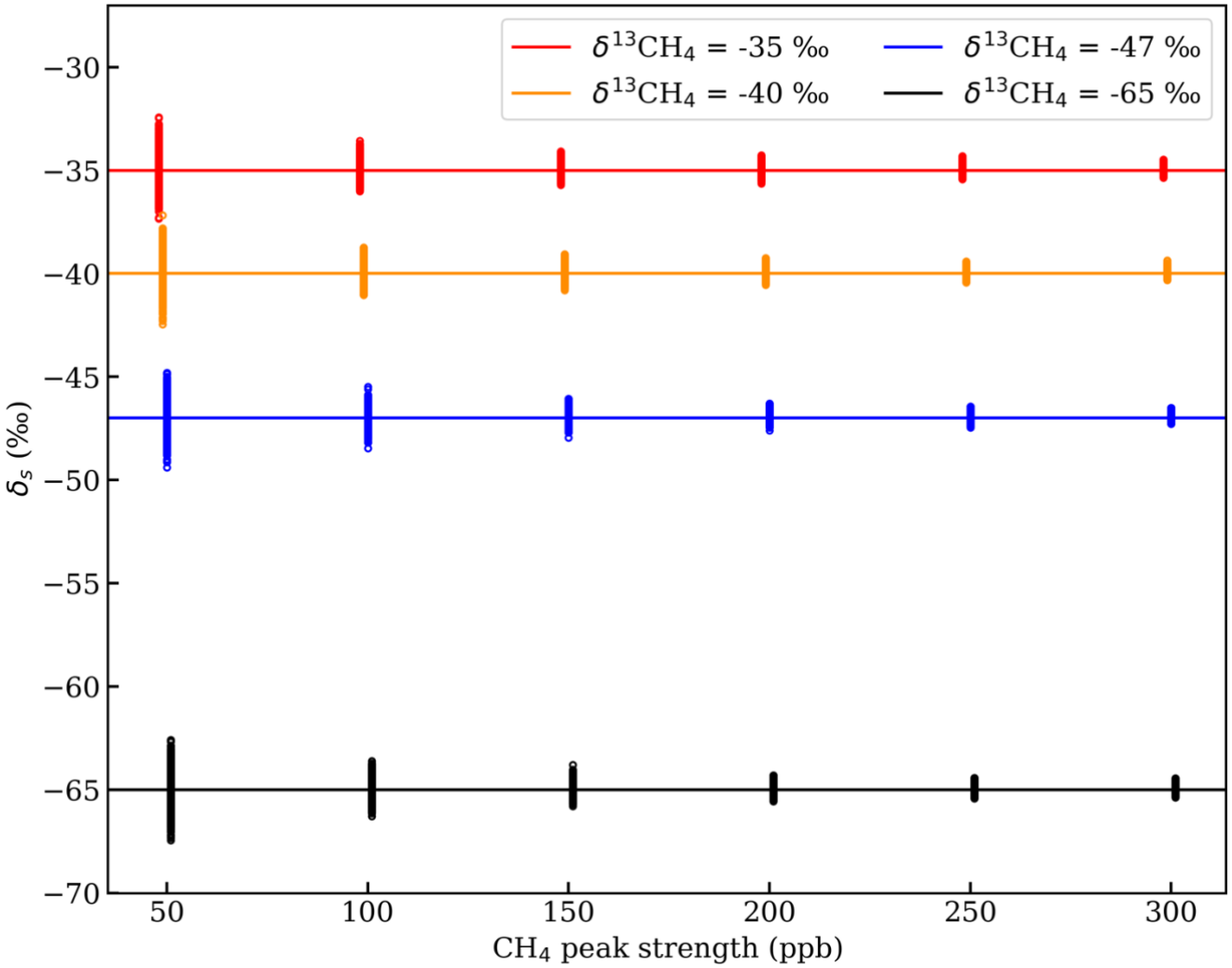

Figure S4: Isotopic source values for ideal pollution events with different isotopic signatures and peak strengths.

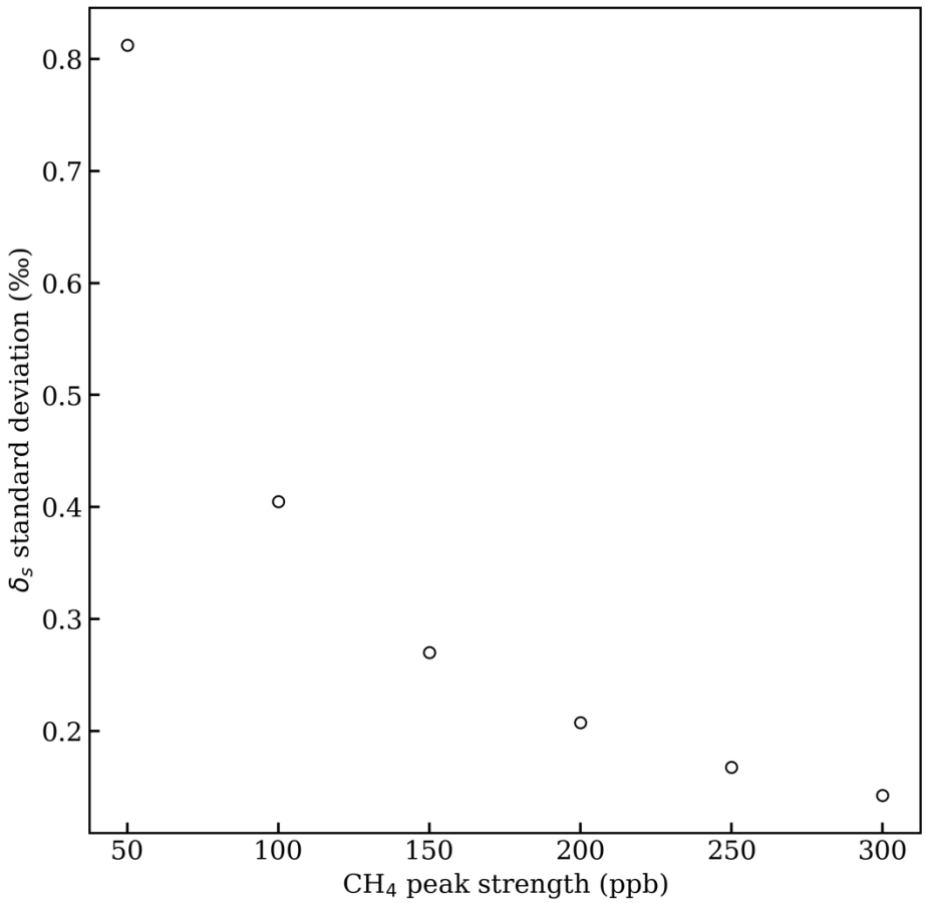

Figure S5: Standard deviations of the recovered isotopic source values for different peak strengths.

Table S1: Pseudo-data peak strength mean and 1σ.

		Pseudo-data peak strength					
		50 ppb	100 ppb	150 ppb	200 ppb	250 ppb	300 ppb
Isotopic signature (δ_s)	-35 ‰	-34.8±0.83	-34.9±0.39	-34.9±0.27	-34.9±0.21	-34.9±0.17	-34.9±0.14
	-40 ‰	-39.9±0.76	-39.9±0.39	-39.9±0.27	-39.9±0.21	-39.9±0.17	-39.9±0.14
	-47 ‰	-46.9±0.81	-46.9±0.41	-46.9±0.27	-46.9±0.20	-46.9±0.16	-46.9±0.15
	-65 ‰	-64.9±0.85	-64.9±0.43	-64.9±0.27	-64.9±0.21	-64.9±0.17	-64.9±0.14

Table S2: Imperial College London isotopic source values summary for different peak strengths and window sizes.

Moving window size	Peak strength (ppb)	Number of δ_s values	Range of δ_s values (‰)	Mean standard error on δ_s (‰)	$\delta_s \leq$ -45 ‰ (%)
12 h	100	1664	[-69.6, -13.2]	3.83	23.7
	150	1046	[-66.3, -24.8]	2.77	24.8
	200	706	[-61.1, -25.6]	2.31	23.9
3-day	100	82	[-65.0, -19.5]	8.02	32.9
	150	41	[-55.8, -28.9]	5.18	36.9
	200	27	[-55.8, -31.1]	4.59	44.4
7-day	100	83	[-60.8, -24.1]	5.57	34.9
	150	47	[-55.2, -27.8]	3.65	31.9
	200	27	[-55.2, -30.9]	3.50	44.4

Simulation and measurement time series for 2018 and 2019

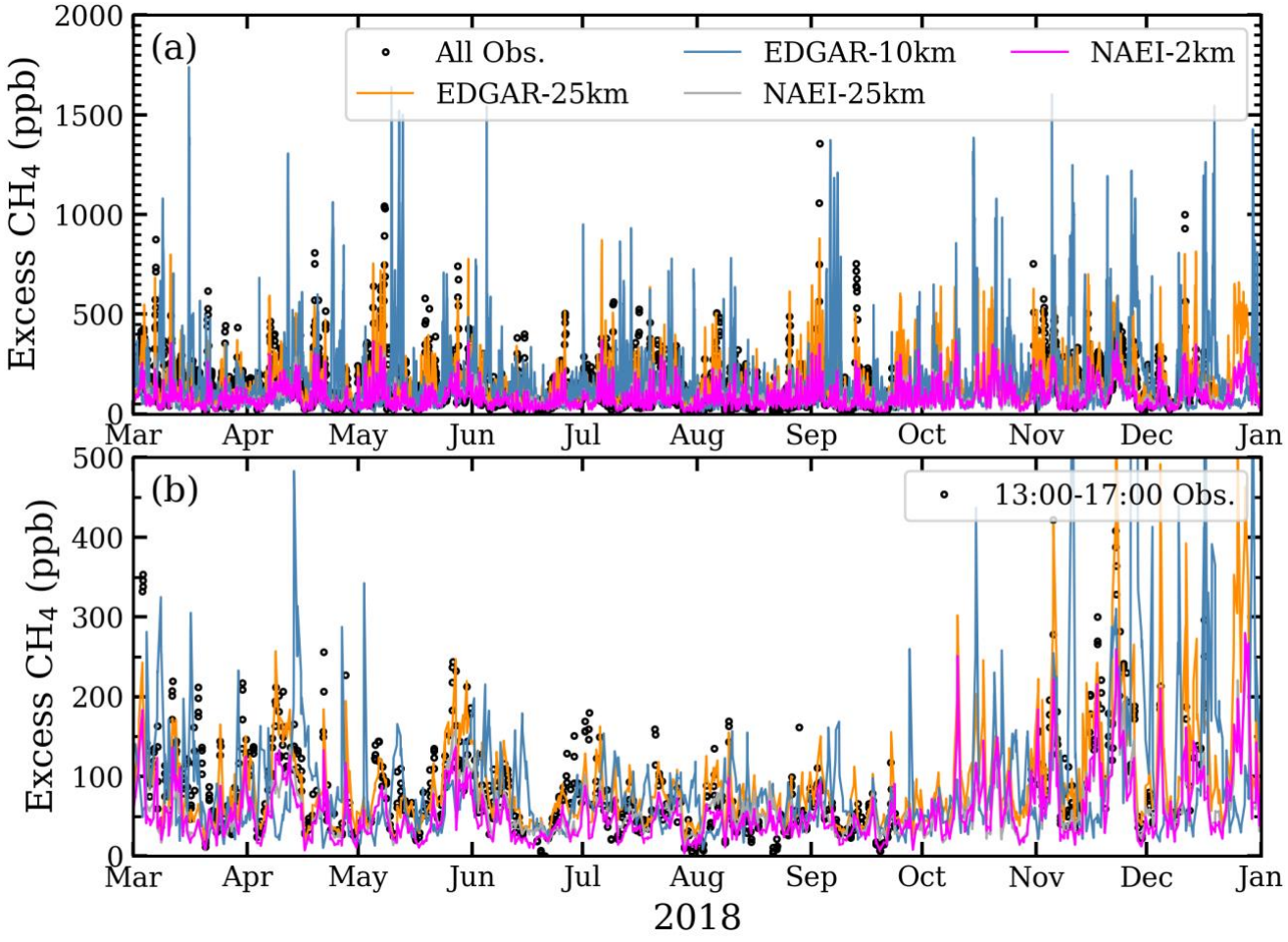

Figure S6: Excess simulated and measured mole fractions for 2018, where the Mace Head background has been subtracted from the observations. (a) shows all data and (b) data from 13:00-17:00.

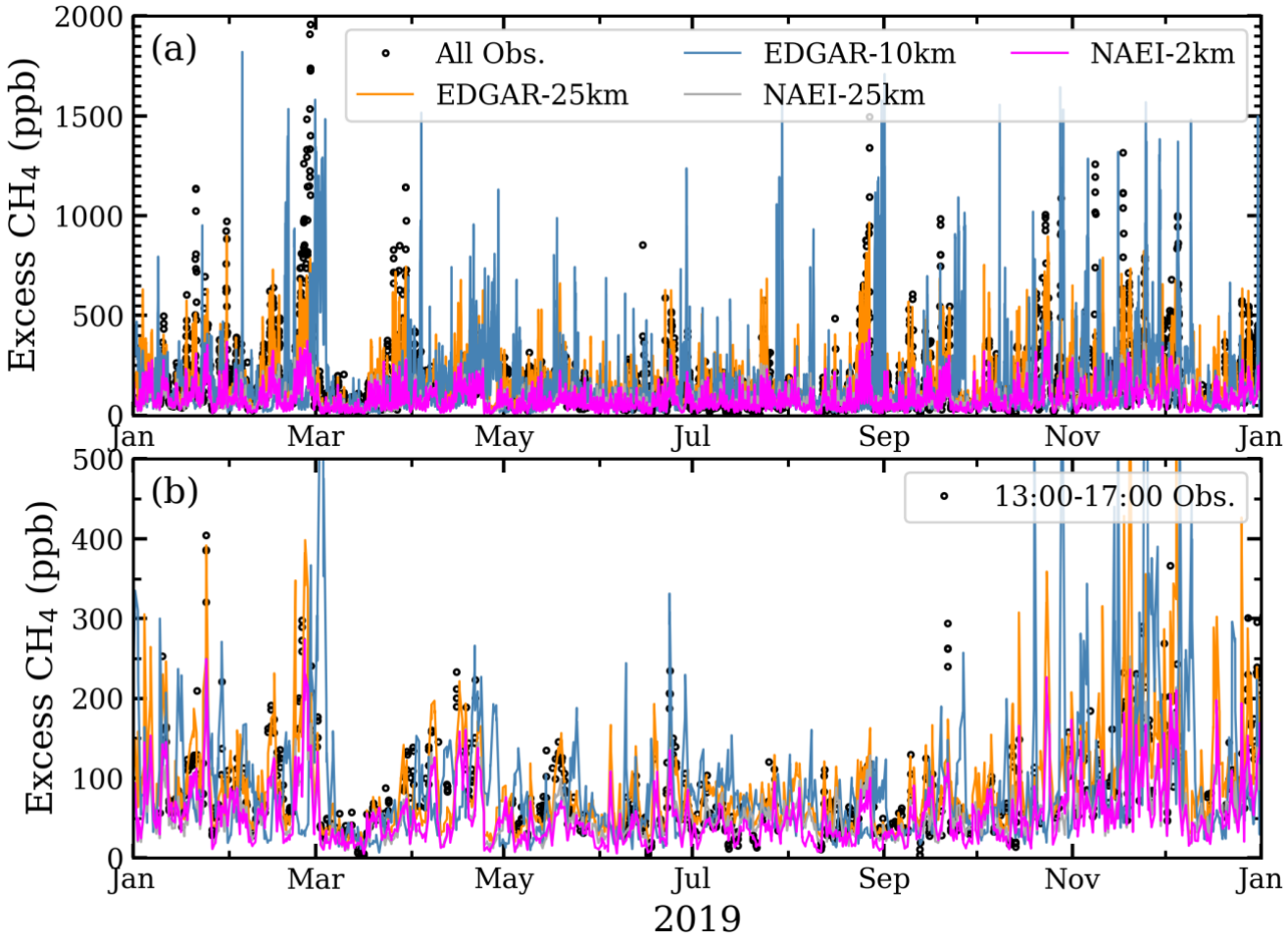

Figure S7: Excess simulated and measured mole fractions for 2019, where the Mace Head background has been subtracted from the observations. (a) shows all data and (b) data from 13:00-17:00.

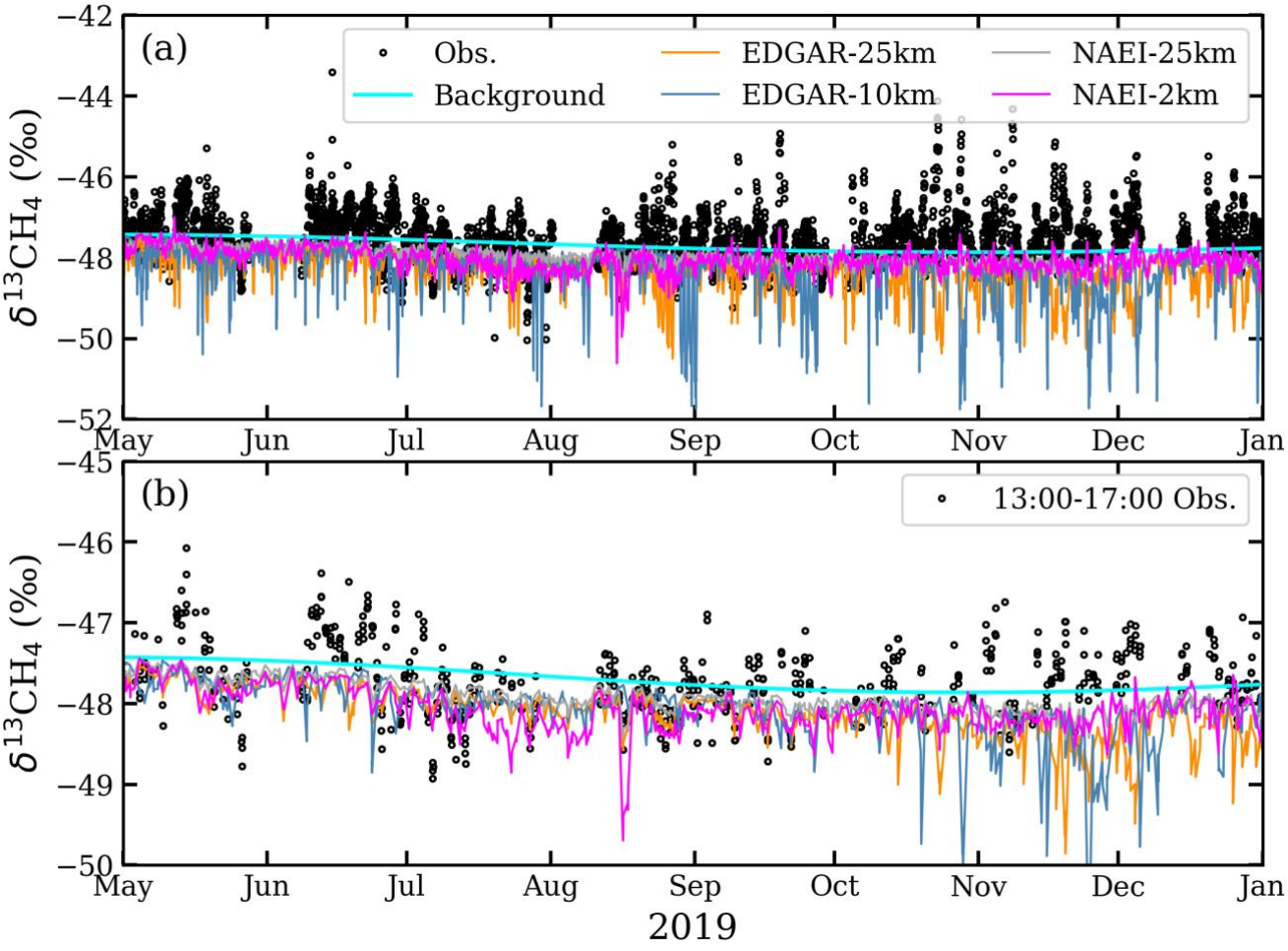

Figure S8: Simulated and measured $\delta^{13}CH_4$ for 2019 using (a) all data and (b) data from 13:00-17:00. The Mace Head background $\delta^{13}CH_4$ is included for reference.

60

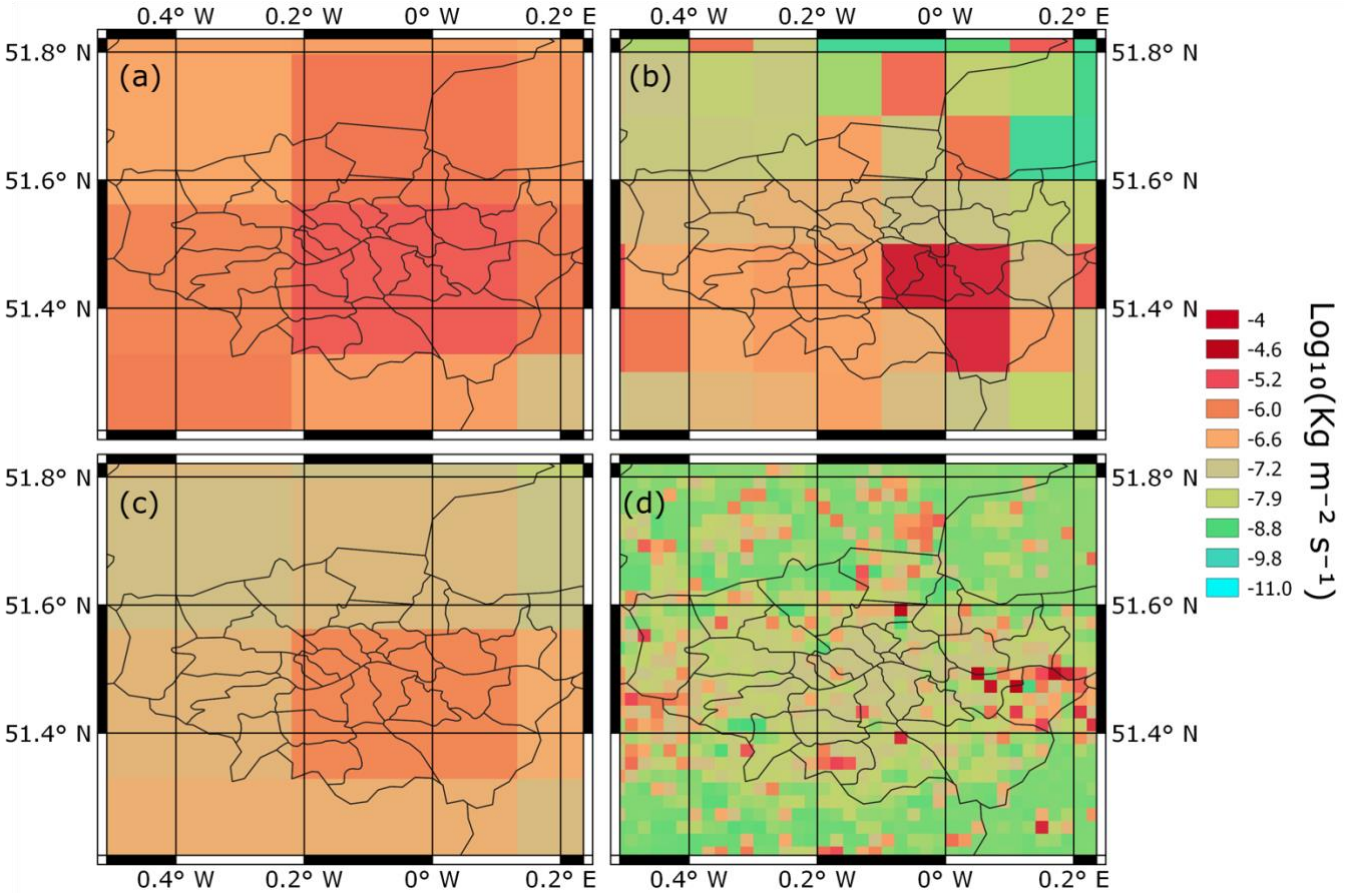

Figure S9: London waste emissions from EDGAR gridded at (a) 0.352º × 0.234º , (b) 0.10º × 0.10º and UK NAEI gridded at (c) 0.352º × 0.234º and (d) 0.02º × 0.02º.

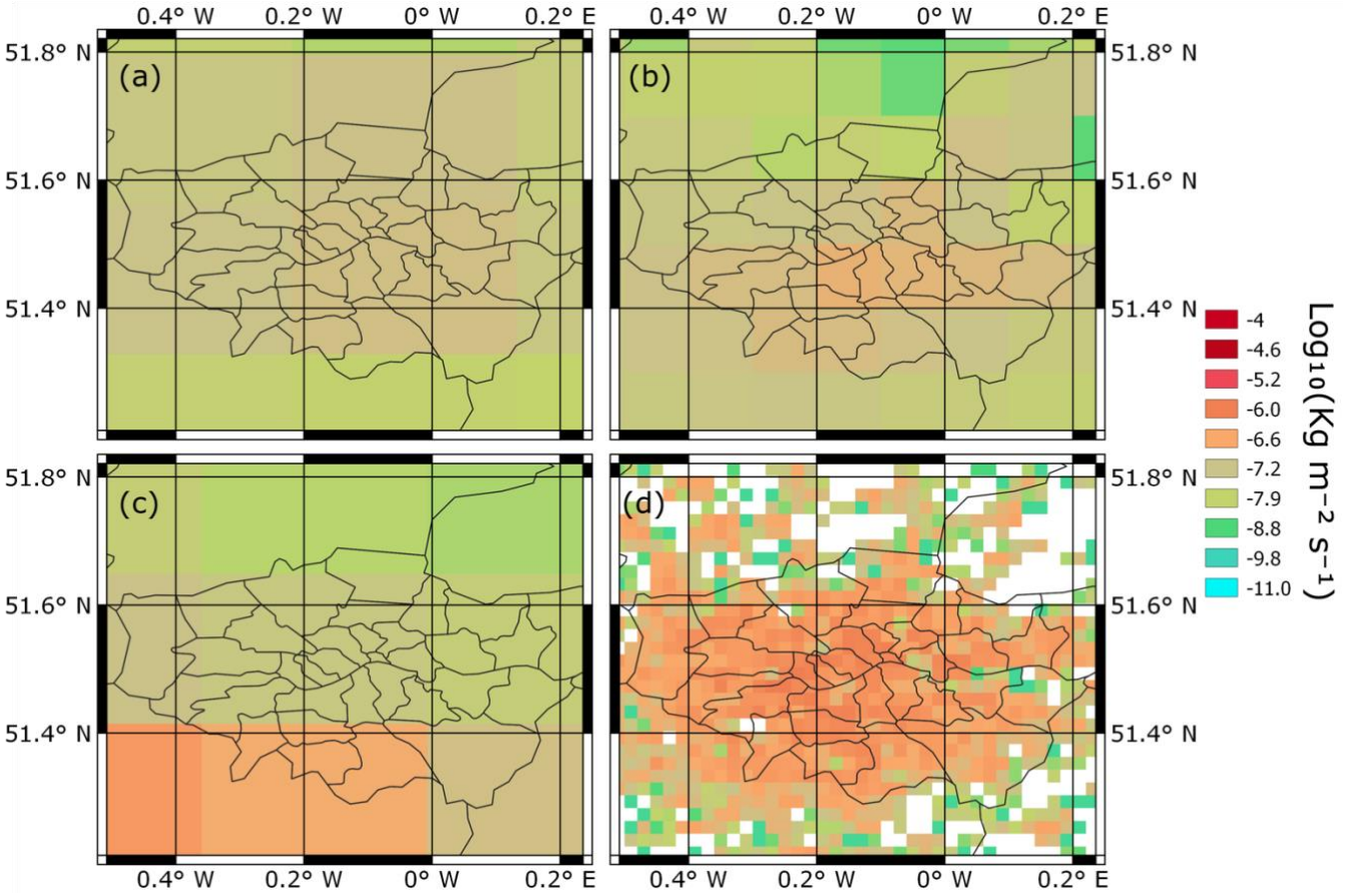

Figure S10: London natural gas emissions from EDGAR gridded at (a) 0.352º × 0.234º , (b) 0.10º × 0.10º and UK NAEI gridded at (c) 0.352º × 0.234º and (d) 0.02º × 0.02º.